ELSEVIER

Journal of Quantitative Spectroscopy & Radiative Transfer 90 (2005) 323–341

Journal of Quantitative Spectroscopy & Radiative Transfer

www.elsevier.com/locate/jqsrt

An inter-comparison of far-infrared line-by-line radiative transfer models

David P. Kratz[a,*], Martin G. Mlynczak[a], Christopher J. Mertens[a], Helen Brindley[b], Larry L. Gordley[c], Javier Martin-Torres[d], Ferenc M. Miskolczi[d], David D. Turner[e]

[a] *Radiation and Aerosols Branch, NASA Langley Research Center, Hampton, VA, USA*
[b] *Space and Atmospheric Physics Group, Imperial College of Science, Technology and Medicine, London, UK*
[c] *G&A Technical Software, Inc., Hampton, VA, USA*
[d] *Analytical Services and Materials, Inc., Hampton, VA, USA*
[e] *Pacific Northwest National Laboratory, Richland, WA, USA*

Received 29 October 2003; accepted 11 April 2004

Abstract

A considerable fraction ($>40\%$) of the outgoing longwave radiation escapes from the Earth's atmosphere-surface system within a region of the spectrum known as the far-infrared (wave-numbers less than 650 cm^{-1}). Dominated by the line and continuum spectral features of the pure rotation band of water vapor, the far-infrared has a strong influence upon the radiative balance of the troposphere, and hence upon the climate of the Earth. Despite the importance of the far-infrared contribution, however, very few spectrally resolved observations have been made of the atmosphere for wave-numbers less than 650 cm^{-1}. The National Aeronautics and Space Administration (NASA), under its Instrument Incubator Program (IIP), is currently developing technology that will enable routine, space-based spectral measurements of the far-infrared. As part of NASA's IIP, the Far-Infrared Spectroscopy of the Troposphere (FIRST) project is developing an instrument that will have the capability of measuring the spectrum over the range from 100 to 1000 cm^{-1} at a resolution of 0.6 cm^{-1}. To properly analyze the data from the FIRST instrument, accurate radiative transfer models will be required. Unlike the mid-infrared, however, no inter-comparison of codes has been performed for the far-infrared. Thus, in parallel with the development of the FIRST instrument, an investigation has been undertaken to inter-compare radiative transfer models for potential use in the analysis of far-infrared measurements. The initial phase of this investigation has focused upon the inter-comparison of six distinct line-by-line models. The results from this study have demonstrated remarkably good agreement among the models, with differences

* Corresponding author. Tel.: +1-757-864-5669; fax: +1-757-864-7996.
E-mail address: david.p.kratz@nasa.gov (D.P. Kratz).

0022-4073/$ - see front matter
doi:10.1016/j.jqsrt.2004.04.006

being of order 0.5%, thereby providing a high measure of confidence in our ability to accurately compute spectral radiances in the far-infrared.

Keywords: Far-infrared; FIRST; Line-by-line; Inter-comparison

1. Introduction

One of the most crucial research endeavors in the field of atmospheric sciences is the improvement of our understanding of the forcings and subsequent feedbacks resulting from changes in the abundances of the infrared-active molecular species in the Earth's atmosphere. For clear-sky conditions, the primary absorber and emitter of thermal infrared radiation is water vapor, which is also one of the most spatially and temporally variable atmospheric trace species. Accurate forecasting of naturally occurring and anthropogenically induced climate changes relies heavily upon determining water vapor's vertical and geographic distribution, as well as correctly characterizing the water vapor spectrum. The far-infrared, specified here to cover the spectral range with wave-numbers less than 650 cm^{-1}, is dominated by the pure rotation band of water vapor, and has been shown to account for over 40% of the energy emitted to space by the Earth's atmosphere-surface system for clear-sky conditions [1]. Recent studies [2–5] have emphasized the crucial contribution that the pure rotation band of water vapor has upon the transfer of far-infrared radiation through the Earth's atmosphere. Most notably, far-infrared water vapor emission has been shown to have a prominent role in determining cooling rates throughout the free troposphere [2]. Moreover, the sensitivity of the outgoing longwave radiation (wave-numbers less than 3000 cm^{-1}) to perturbations in upper tropospheric humidity has been found to be greatest in the far-infrared [6].

Even though far-infrared radiation strongly influences the Earth's thermal energy budget, there are currently no operational satellite instruments that are capable of directly measuring the spectrally resolved radiant energy emitted by the Earth's atmosphere-surface system for wave-numbers less than 650 cm^{-1}. To correct this deficiency, the Far-Infrared Spectroscopy of the Troposphere (FIRST) project, within the framework of the National Aeronautics and Space Administration (NASA) Instrument Incubator Program (IIP), is developing an instrument that will have the capability of measuring the spectrum over the range from 100 to 1000 cm^{-1} at a resolution of 0.6 cm^{-1}.

To better prepare for the analysis of the far-infrared measurements once they became available, a Science Advisory Team (SAT) was created as part of the FIRST project to perform inter-comparisons of line-by-line radiative transfer model calculations for the far-infrared spectral region from 100 to 650 cm^{-1}. Previous inter-comparison initiatives have compared the broadband infrared [7] or mid-infrared [8], but have not specifically examined the far-infrared. The initial set of far-infrared calculations, as reported in this study, involve a series of radiance calculations performed at a resolution of 1 cm^{-1}, a resolution comparable to the resolution of the FIRST instrument. The calculations utilize a set of hydrostatically consistent atmospheric profiles that are used to investigate the performance of the individual line-by-line models and to examine the impact of altering the inputs into the models, e.g., line parameters and continuum formulations.

A brief review of the FIRST project, presented in the next section, is followed by a discussion of the background material necessary to perform the calculations in the inter-comparison study. The discussion continues with brief synopses of the participating models. Results are then presented for the inter-comparison among the different models as well as the inter-comparison among the various inputs into a single model. The final section provides concluding remarks along with a brief description of future plans to expand the scope of this inter-comparison.

2. The FIRST project

The goal of the FIRST project is to develop and field demonstrate a nadir-viewing instrument capable of measuring electromagnetic energy over the spectral range from 100 to 1000 cm^{-1} with an unapodized spectral resolution of 0.6 cm^{-1}. This spectral coverage and resolution are required to measure the unobserved far-infrared while simultaneously determining temperature from the CO_2 15 μm band. The spectral coverage beyond the far-infrared, i.e., between 650 and 1000 cm^{-1}, is required for the inter-comparison of calibrated radiances against existing mid-infrared sensors where known absolute calibration standards exist. The FIRST instrument is designed to record a complete spectrum every 1.2 s. To achieve these goals, the FIRST project has focused on the development of broad spectral bandpass beamsplitters, detector focal planes, and a high throughput Fourier transform spectrometer [9]. The FIRST instrument is the predecessor of a space-based sensor that will have an instantaneous field-of-view of 10 km from an altitude of 900 km and that will employ cross-track scanning to enable daily global coverage [10].

Preliminary calculations [1] have emphasized the value of far-infrared measurements by demonstrating that the (100–650 cm^{-1}) portion of the spectrum is responsible for over 40% of the outgoing thermal energy emitted by the Earth's atmosphere and surface. Additional calculations have further demonstrated that the Earth's outgoing far-infrared spectrum is strongly affected by water vapor [1–4,11] and cirrus clouds [12]. Thus, as part of the FIRST project, the SAT was formed to conduct the inter-comparison of radiative transfer codes for the far-infrared. The results of this effort should enable a more effective analysis of the far-infrared data once it becomes available.

3. Background

One of the most challenging aspects of any model inter-comparison is having sufficient information to clearly distinguish between the inherent differences among the models and the inputs into those models. To minimize such complications, we have specified a number of the input parameters to be included in the study, such as the atmospheric profiles of temperature, pressure, and the mixing ratios of the molecular species. We have also specified the vertical resolution, the surface emissivity, and the sky conditions. There remain, however, other model inputs which were not constrained, specifically the molecular absorption parameters and continuum formulations. Instead, this study only required that those input parameters be clearly identified so that one of the other models in the study could use the same inputs, and thus provide a valid comparison.

3.1. Atmospheres

Three atmospheric profiles, tropical, sub-arctic winter and isothermal, have been created for the far-infrared radiative transfer code inter-comparison. These atmospheric profiles are hydrostatically consistent and represent highly diverse atmospheric conditions, and therefore, provide stringent test cases for the inter-comparison. The tropical and sub-arctic winter profiles are based upon the FASCODE [13] versions of the McClatchey et al. atmospheres [14]. The isothermal profile uses the surface temperature and pressure from the FASCODE US Standard atmosphere, since this atmospheric profile has a surface temperature which is very near the mean global surface temperature of 288 K. The temperature of the atmosphere for the isothermal case is taken to be 255 K, consistent with the effective temperature of the atmosphere computed from a zero-dimensional radiative equilibrium calculation, assuming a 30% average Earth albedo and a solar constant of 1368 W m^{-2}. The vertical resolution for all three profiles has been taken to be 1 km throughout the entire atmosphere from the surface at 0 km to the top of atmosphere (TOA) at 70 km. For the present calculations, three species profiles have been included: H_2O, CO_2, and O_3.

3.2. Spectral databases

All of the participating models in this study obtained their molecular absorption parameters from one of the HITRAN databases, with most using the 2000 version [15] and one using the 1996 version [16]. Since the differences between calculations using the 1996 and 2000 databases could easily be taken into account, no requirement was made to upgrade all the models to the HITRAN 2000 database.

3.3. Continuum models

In the initial phases of this study several different continuum formulations were employed. Significant disagreement among the models, however, quickly led to the adoption of the CKD continuum codes [17]. Most of the participating models had either already begun using or could quickly adopt version 2.4 of the CKD code, although one of the models continued to use version 2.1 of the CKD code. As with the differences between the two HITRAN databases, the differences between the two CKD codes could easily be taken into account. Nevertheless, there are significant differences in the far-infrared portion of the spectrum between versions 2.1 and 2.4 of the CKD code [see e.g., Tobin et al. [5] and Kratz [1]. Indeed, spectral measurements extending to 380 cm^{-1} revealed a significant discrepancy between the theoretical (CKD version 2.2) and observed far-infrared water vapor continuum [5]. These measurements led directly to revision of the continuum code (CKD version 2.3) [18].

3.4. Instructions to participants

Since the FIRST project is principally concerned with the 100–650 cm^{-1} spectral range, and studies related to the Inter-comparison of Radiation Codes and Climate Models (ICRCCM) [7] endeavor had already compared theoretical models with Atmospheric Emitted Radiance Interferometer (AERI) data [19] for the spectral range from 550 to 3000 cm^{-1} (see e.g., Turner et al. [20]), our

far-infrared calculations examined only the spectral range from 100 to 650 cm^{-1}. The participants were requested to provide the following values: wave-number for each spectral interval, upward nadir radiance from the surface, upward nadir radiances at the top of the atmosphere (taken to be 70 km) and downward zenith radiances to the surface for the tropical, subarctic winter, and isothermal atmospheres using the hydrostatic atmospheric profiles provided. Radiance calculations were chosen to avoid the complications of angular integration. The calculations were required to span the entire spectral range from 100 to 650 cm^{-1} and to be provided at a spectral resolution of 1 cm^{-1} (centered on the 0.5 cm^{-1} value). The choice of spectral resolution for the calculations was driven by the proposed design of the FIRST instrument which was anticipated to have a spectral resolution of approximately 1 cm^{-1}. Each calculation was required to include the molecular species: H_2O, CO_2, and O_3, as well as the H_2O continuum, and were to be run for clear-sky conditions with the surface emissivity taken to be unity. Participants were requested to specify which line parameter database (e.g., HITRAN 2000) and which H_2O continuum model (e.g., CKD 2.4) were used, and whether or not line mixing was taken into consideration.

A word of caution was issued concerning the isothermal atmosphere. Since this profile possesses a large, 33.2 K, temperature discontinuity at the surface boundary, a substantial discrepancy in the radiances would result if the profile was improperly treated. The relatively warm surface temperature only directly contributes to the emission from the surface, and does not contribute to the temperature of lowest layer of the atmosphere. The energy emitted from the relatively warm surface does, however, pass through the relatively cool atmosphere and thereby affects the outgoing TOA emission spectrum.

4. Participating radiative transfer model descriptions

Six distinct radiative transfer algorithms have participated in the initial phase of the far-infrared inter-comparison effort. The Line-By-Line Radiative Transfer Model (LBLRTM), developed at Atmospheric and Environmental Research Inc., was designed to achieve high accuracy with computational efficiency [2,21], and has been used extensively for a variety of applications [20,22–25]. LINEPAK, developed at G&A Technical Software Inc., was designed as a modular set of subroutines that could be easily assembled to compute absorption cross sections, transmission functions, and various moments of the atmospheric radiation transfer equation [26], and has been used to investigate the application of far-infrared observations to retrievals of upper tropospheric water vapor [27]. The High-resolution Atmospheric Radiative Transfer Code (HARTCODE), developed at the International Centre for Theoretical Physics, Trieste, Italy, was created to produce calculations where the numerical accuracy of the spectral atmospheric transmittance and radiance computations were kept under strict control [28]. The FUll Transfer By Ordinary LINe-by-line (FUTBOLIN) algorithm, developed initially as an academic exercise, was created to be a flexible radiative transfer code to calculate atmospheric emission/transmission spectra for planetary atmospheres [29,30]. The General Line-by-line Atmospheric Transmittance and Radiance Model (GENLN2) line-by-line model, developed by D.P. Edwards while associated with the Hooke Institute at Oxford University and the National Center for Atmospheric Research, was created to provide a flexible, computationally efficient radiative transfer code [31]. GENLN2 has a clear modular structure and a transparent physical basis, allowing the model to be easily adapted for specific research needs [11,32,33]. The Monochromatic Radiative

Transfer Algorithm (MRTA), developed at the SUNY at Stony Brook in the 1980s to examine the radiative effects of infrared-active gases in planetary atmospheres, has since been used for minor trace gas radiative forcing calculations [34], for the production of correlated k-distributions for satellite channels [35], for high resolution modeling of the far-infrared [1], and for establishing the stability of satellite instruments [36]. The present inter-comparison, therefore, truly represents a test of the accuracies of different formulations rather than different applications of a single technique.

5. Results

To facilitate an inter-comparison of the model calculations for the spectral range from 100 to 650 cm^{-1}, the results from each model were subtracted from the results of a single reference model. Even though LBLRTM and GENLN2 have been established as standard references, we found that accommodating algorithmic and input differences among the models in the current study was more straightforward by using MRTA as the reference.

Fig. 1 illustrates an inter-comparison of the TOA (upper plot) and surface (lower plot) radiance calculations from the different radiative transfer codes for the tropical atmosphere. The uppermost curve in each plot represents either the outgoing TOA nadir radiance or the downward surface zenith radiance as calculated with MRTA using the HITRAN 2000 database for H_2O, CO_2, and O_3, and version 2.4 of the CKD continuum code. The numbered curves represent: (1) LBLRTM-MRTA, (2) LINEPAK-MRTA, (3) HARTCODE-MRTA, (4) FUTBOLIN-MRTA, and (5) GENLN2 v3-MRTA. To distinguish among the different inter-comparisons, the results have been offset vertically by 0.01, 0.005, 0.0, −0.005, and −0.01 W m^{-2} sr^{-1} $(cm^{-1})^{-1}$, respectively. In both the TOA and surface cases, the differences among the models are quite small, with the normalized radiances defined by

$$R_\omega = \frac{I_\omega(Model) - I_\omega(MRTA)}{I_\omega(MRTA)} \tag{1}$$

having means and standard deviations that are less than 0.40%. In Eq. (1) the variable, I_ω(MRTA), is the radiance calculated using MRTA at wave number ω, while I_ω(Model) is the radiance calculated using any of the other five models. The only notable, albeit small, discrepancy is with HARTCODE which produces slightly lower (−0.37%) outgoing TOA normalized radiances and slightly greater (0.27%) downward surface normalized radiances when compared with MRTA. This difference has been attributed to an atmospheric emission that is produced from a somewhat lower altitude in the HARTCODE calculation. An inter-comparison of the integrated radiances defined to be

$$I(Model) = \int_{100}^{650} I_\omega(Model)\,\mathrm{d}\omega \tag{2}$$

and calculated over the entire 100–650 cm^{-1} spectral range for the tropical atmosphere is presented in Table 1. As anticipated from Fig. 1, the results for the integrated radiances demonstrate excellent agreement among the models with the largest integrated difference being less than 0.5%.

Fig. 2 illustrates an inter-comparison of the TOA and surface radiance calculations for the sub-arctic winter atmosphere using the same format as Fig. 1. As with the tropical atmosphere, the differences among the models are quite small with the normalized radiances having means that are less than 0.36% and standard deviations that are less than 0.83%. The most persistent, albeit small, deviation involves LINEPAK which produces somewhat less emission to the surface within the

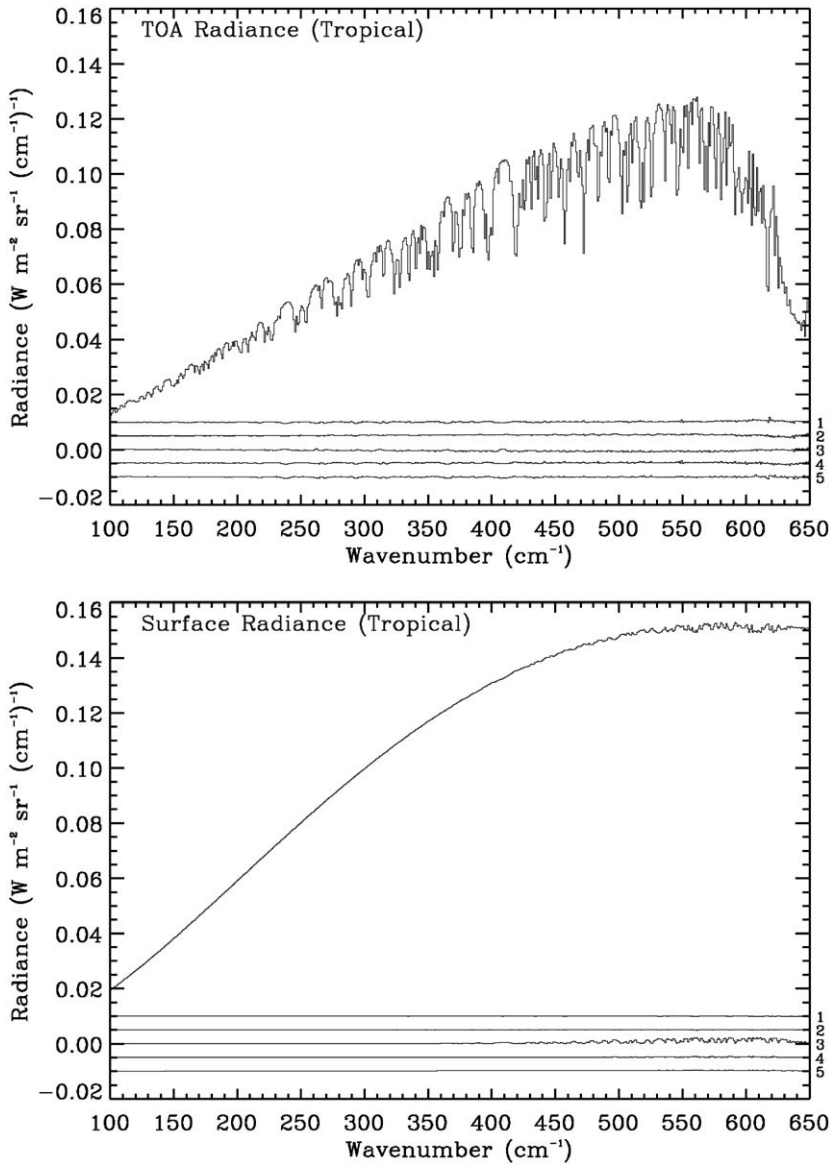

Fig. 1. A comparison of TOA and surface radiance calculations for the tropical atmosphere for the spectral range from 100 to 650 cm^{-1}. The uppermost curve represents the radiances as calculated with the MRTA using the HITRAN 2000 database for H_2O, CO_2, and O_3, and version 2.4 of the CKD continuum. The numbered curves represent: (1) LBLRTM-MRTA, (2) LINEPAK-MRTA, (3) HARTCODE-MRTA, (4) FUTBOLIN-MRTA, and (5) GENLN2 v3-MRTA.

pseudo-windows regions, e.g., at 479, 489 and 497 cm^{-1}. If the LINEPAK results are removed from the inter-comparison, the means and standard deviations for the normalized radiances fall to 0.23% and 0.45%, respectively. The locations of the LINEPAK deviations suggest a modeling difference involving the handling of the continuum. Several other differences can be seen in Fig. 2, most

Table 1
Comparison of integrated radiances (W m^{-2} sr^{-1}) calculated for the spectral range from 100 to 650 cm^{-1} (comparisons include the effects of H_2O, CO_2, O_3, and the continua of H_2O and CO_2)

Model	I_{up} (Surface)	I_{up} (TOA)	I_{dn} (Surface)
Tropical atmosphere			
MRTA	60.338	39.962	60.089
LBLRTM-MRTA	−0.015	0.030	0.000
LINEPAK-MRTA	0.011	0.111	0.015
HARTCODE-MRTA	0.006	−0.184	0.220
FUTBOLIN-MRTA	0.011	0.085	0.032
GENLN2 v3-MRTA	0.013	0.027	0.100
Subarctic winter atmosphere			
MRTA	41.047	34.513	35.869
LBLRTM-MRTA	0.005	0.034	−0.034
LINEPAK-MRTA	0.008	0.071	−0.100
HARTCODE-MRTA	0.004	−0.073	−0.007
FUTBOLIN-MRTA	0.007	0.070	0.037
GENLN2 v3-MRTA	0.009	0.036	0.046
Isothermal atmosphere			
MRTA	54.858	42.646	34.338
LBLRTM-MRTA	−0.166	−0.006	0.037
LINEPAK-MRTA	0.010	0.081	−0.170
HARTCODE-MRTA	0.005	0.008	−0.004
FUTBOLIN-MRTA	0.009	−0.027	0.094
GENLN2 v3-MRTA	0.011	−0.019	0.082

notably HARTCODE, which has a slightly greater emission to the surface around the 410 cm^{-1} region. These differences, however, tend to be very small. An inter-comparison of the integrated radiances calculated for the sub-arctic winter atmosphere is presented in Table 1. As before, the results for the integrated radiances demonstrate excellent agreement among the models with the largest integrated difference being less than 0.3%.

Fig. 3 illustrates an inter-comparison of the TOA and surface radiance calculations for the isothermal atmosphere using the same format as Fig. 1. As with the tropical and sub-arctic winter atmospheres, the differences among the models for the TOA calculations for the isothermal atmosphere are extremely small. The downward surface radiances for the isothermal atmosphere, however, did prove to be somewhat more sensitive to model differences. Indeed, although the isothermal case was anticipated to be the most straightforward, the large temperature discontinuity at the surface caused some significant challenges. Once these challenges were overcome, however, the differences among the models were found to be quite small, with the normalized radiances having means that are less than 0.62% and standard deviations that are less than 1.19%. Analogous to the sub-arctic winter atmosphere, LINEPAK produces somewhat less emission to the surface within the pseudo-windows regions, and again if the LINEPAK results are removed from the inter-comparison, the means and standard deviations for the normalized radiances are significantly reduced, in this case to 0.32%

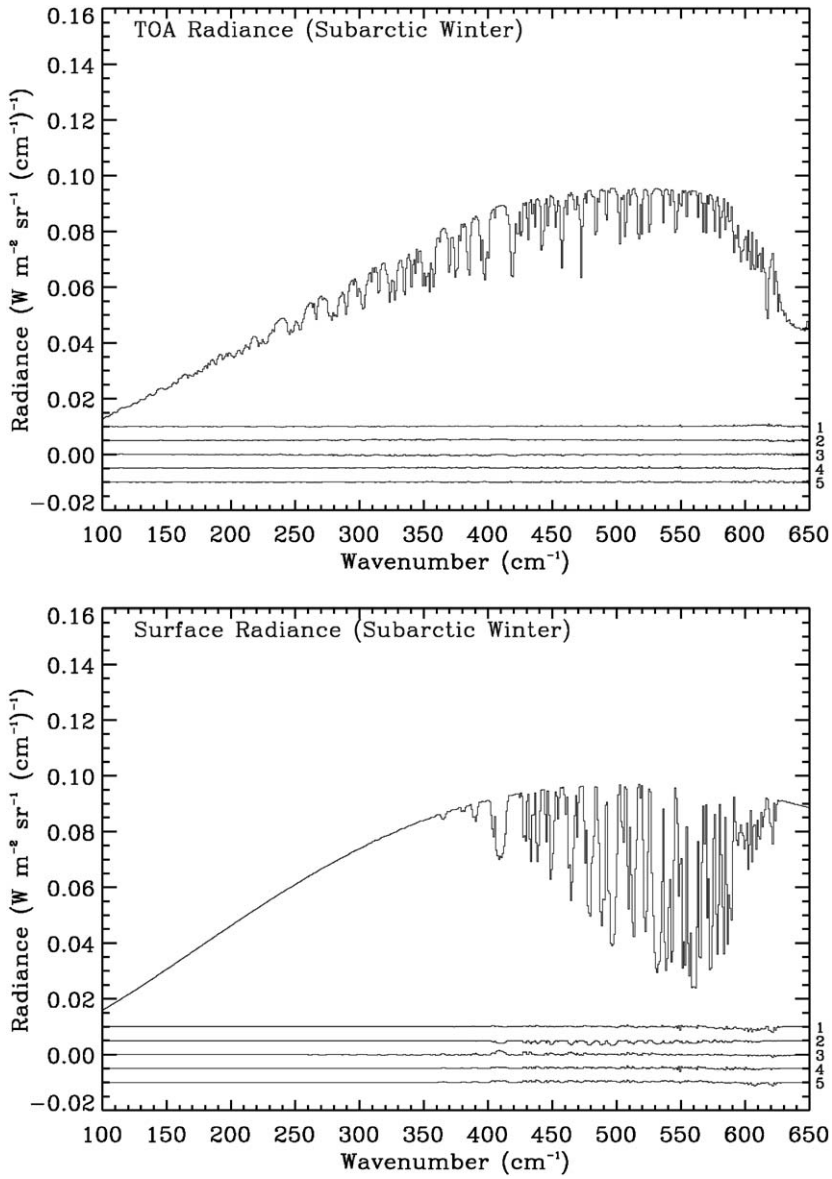

Fig. 2. A comparison of TOA and surface radiance calculations analogous to those presented in Fig. 1 except this case is for the sub-arctic winter atmosphere.

and 0.66%, respectively. As noted previously, the locations of the deviations involving LINEPAK suggest a modeling difference involving the handling of the continuum. LBLRTM, FUTBOLIN and GENLN2 also produce differences which are somewhat similar to those produced by LINEPAK, although their emissions to the surface are opposite in sign, i.e., being somewhat greater rather than less within the pseudo-windows regions. The locations of these deviations again suggest a

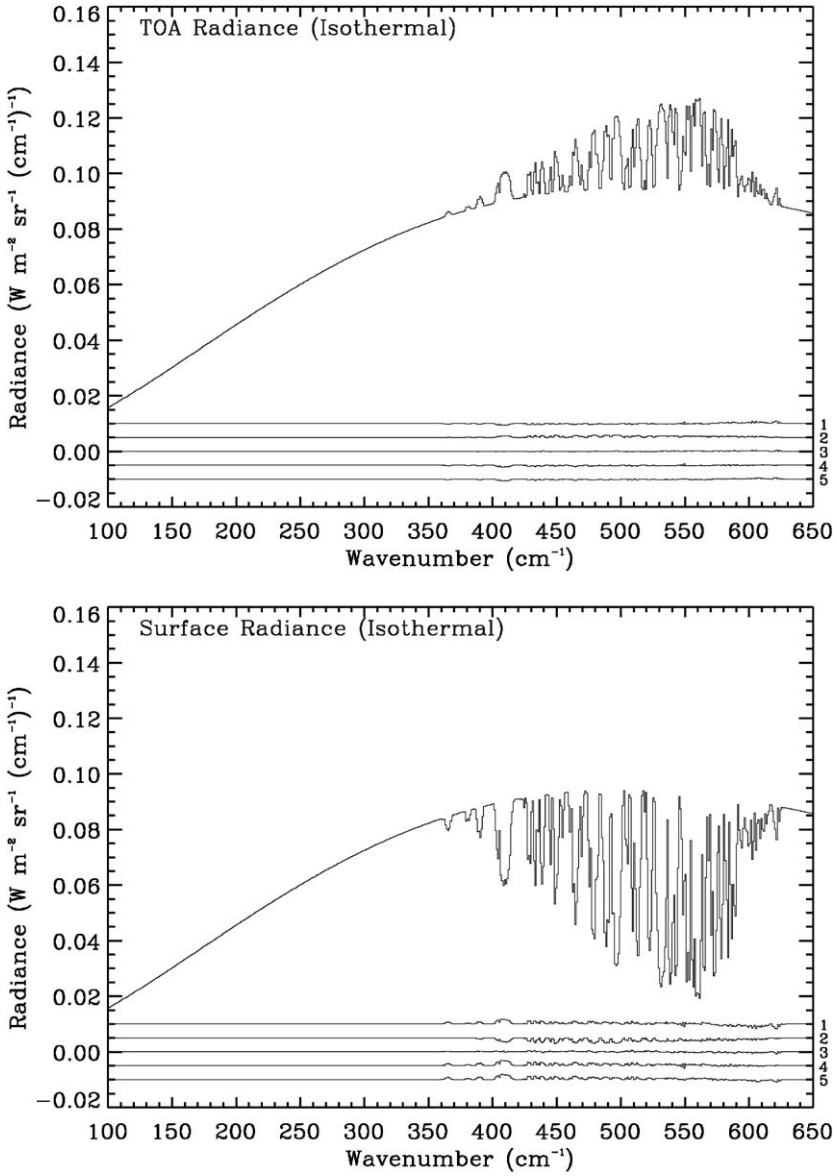

Fig. 3. A comparison of TOA and surface radiance calculations analogous to those presented in Fig. 1 except this case is for the isothermal atmosphere.

modeling difference involving the continuum. The best agreement for the isothermal atmosphere, including inter-comparisons among the LBLRTM, FUTBOLIN and GENLN2 models, is between HARTCODE and MRTA. An inter-comparison of the integrated radiances calculated for the isothermal atmosphere is presented in Table 1. As can be seen from the results for the integrated radiances, despite some slightly enhanced spectral sensitivity, the agreement among the models for the integrated radiances is still excellent with the largest difference being less than 0.5%.

To gain a better perspective on the magnitude of the differences observed in the model inter-comparison, an additional series of calculations was performed to test how changing the model inputs affected the MRTA results. While a considerable number of test cases could be run, the present study focused upon six specific cases that either were encountered or were expected to be encountered. Case (1) considered the radiative impact of neglecting CO_2 line mixing. Despite being a potentially important component of CO_2 absorption and emission, line mixing is frequently neglected in model calculations. Case (2) considered the impact of neglecting N_2O absorption and emission. To avoid questions concerning the composition of the atmosphere, the present study requested that only H_2O, CO_2, O_3 and the continuum be included in the model calculations. Case (3) considered the impact of using a Planck function dependent upon a path-weighted temperature to represent the emission from each atmospheric layer. Case (4) examined the differences between versions 2.1 and 2.4 of the CKD continuum code. Case (5) examined the differences between the 1996 and 2000 HITRAN databases. Case (6) examined the differences between the CKD 2.4 and the recently released MT_CKD [37] 1.0 continuum codes.

Fig. 4 illustrates an inter-comparison of the TOA (upper plot) and surface (lower plot) radiance calculations for the tropical atmosphere using MRTA for the test cases described in the previous paragraph. The uppermost curve in each plot represents either the outgoing TOA nadir radiance or the downward surface zenith radiance as calculated with MRTA using the HITRAN 2000 database for H_2O, CO_2, O_3, N_2O, and version 2.4 of the CKD continuum code. The numbered curves represent differences due to: (1) the removal of CO_2 line mixing, (2) the removal of N_2O absorption, (3) substitution of a mean-layer temperature Planck function for the linear in τ approximation [38], (4) substitution of CKD 2.1 for CKD 2.4, (5) substitution of HITRAN 1996 for HITRAN 2000, and (6) substitution of MT_CKD 1.0 for CKD 2.4. To distinguish among the different inter-comparisons, the results have been offset vertically by 0.01, 0.005, 0.0, −0.005, −0.01, and -0.015 W m^{-2} sr^{-1} (cm^{-1})$^{-1}$, respectively.

The comparisons for the TOA radiances illustrate several notable discrepancies for the tropical atmosphere. For instance, neglecting the CO_2 line mixing results in a significant (14%) underestimation of the outgoing radiance at 618.5 cm^{-1}, while neglecting N_2O results in a significant (35%) overestimation of the outgoing radiance at 589.5 cm^{-1}. These discrepancies, however, are confined to rather small spectral ranges, and therefore, the differences in the integrated radiances (see Table 2) are only −0.07% and 0.29%, respectively. From an energy balance viewpoint, a more important case (case 4) involves the substitution of the CKD 2.1 for the CKD 2.4 continuum, which causes the atmosphere to be somewhat more opaque in the 230–500 cm^{-1} spectral range, resulting in the integrated TOA radiance being reduced by 0.95%. The effect of substituting the MT_CKD 1.0 for the CKD 2.4 continuum is similar in appearance but smaller in magnitude than the substitution of the CKD 2.1 for the CKD 2.4 continuum and results in a reduction of the integrated TOA radiance by 0.21%. Replacing the HITRAN 2000 database with the HITRAN 1996 database produces a slightly more transparent atmosphere in the 500–600 cm^{-1} spectral range, resulting in the integrated TOA radiance being increased by 0.16%. In contrast, the downward radiances to the surface are found to be insensitive to nearly all of these modifications. The exception to this trend involves case 3 where the emission within each layer is approximated by a mean-layer temperature Planck function. For this case, there is minimal impact upon the TOA radiance; however, there is more than a 2.0% decrease in the integrated emission to the surface, a difference which is over 4 times greater than any of the differences in the model inter-comparisons shown in Table 1. As a

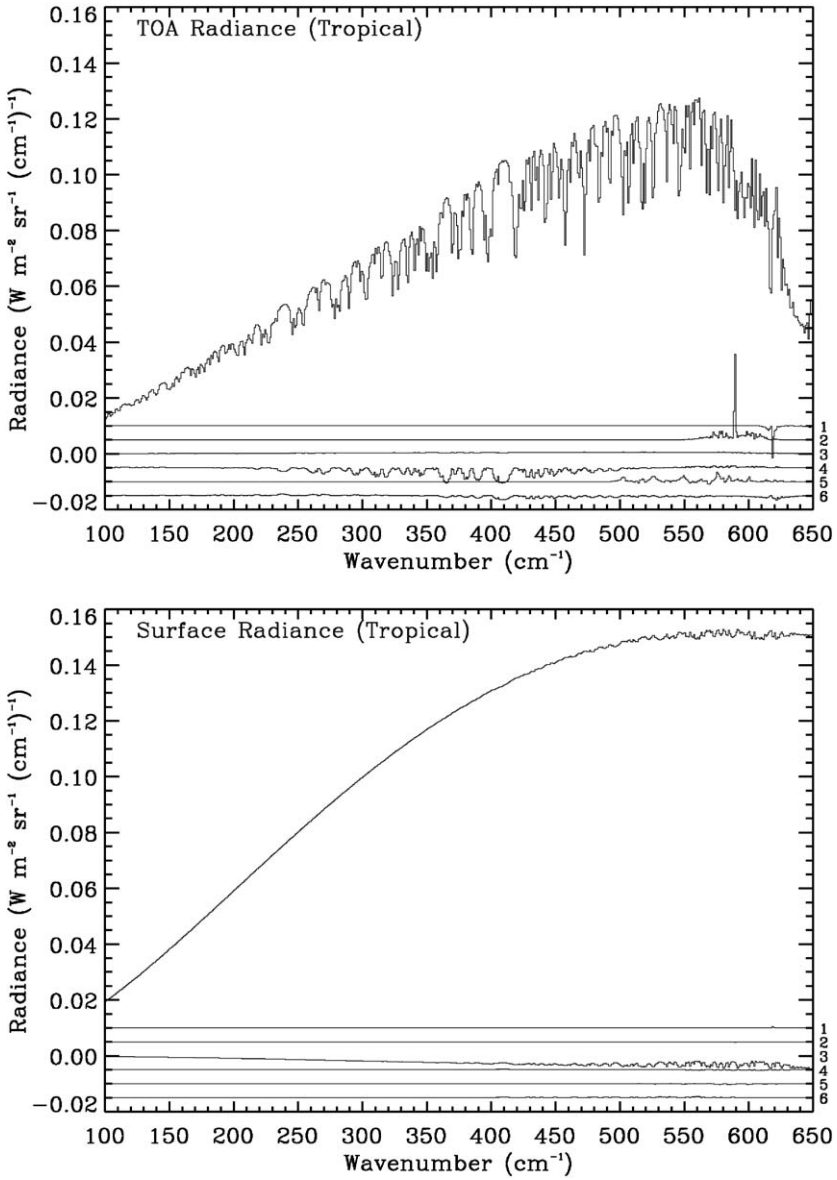

Fig. 4. A comparison of TOA and surface radiance calculations for the tropical atmosphere for the spectral range from 100 to 650 cm^{-1}. The uppermost curve represents the radiances as calculated by the MRTA using line mixing, the HITRAN 2000 database for H_2O, CO_2, O_3 and N_2O, and version 2.4 of the CKD continuum. The numbered curves represent MRTA calculations: (1) without line mixing–with line mixing, (2) without N_2O–with N_2O, (3) the mean-layer temperature Planck function layer approximation—linear in τ approximation, (4) CKD 2.1–CKD 2.4, (5) HITRAN 1996–HITRAN 2000, and (6) MT_CKD 1.0–CKD 2.4.

further test of the methods available to determine the emission within a layer, we compared the linear in τ method [38] to the 1 and 2 term Padé approximations for the linear in τ method [2] and to the exponential in τ method [39]. The differences among these methods were more than an order

Table 2
Comparison of integrated radiances (W m^{-2} sr^{-1}) calculated for the spectral range from 100 to 650 cm^{-1}

Model	I_{up} (Surface)	I_{up} (TOA)	I_{dn} (Surface)
Tropical atmosphere			
MRTA with lm + N_2O	60.338	39.847	60.089
w/o-w linmix	0.000	−0.028	0.001
w/o-w N_2O	0.000	0.115	0.000
Mid-layer T-lin τ	0.000	0.167	−1.218
CKD2.1–CKD2.4	0.000	−0.377	0.003
HITRAN '96–2k	0.000	0.063	−0.010
MT_CKD–CKD2.4	0.000	−0.085	0.018
Subarctic winter atmosphere			
MRTA with lm + N_2O	41.047	34.434	35.973
w/o-w linmix	0.000	−0.016	0.019
w/o-w N_2O	0.000	0.079	−0.104
Mid-layer T-lin τ	0.000	0.071	0.161
CKD2.1–CKD2.4	0.000	−0.307	0.473
HITRAN '96–2k	0.000	0.020	−0.141
MT_CKD–CKD2.4	0.000	−0.031	0.210
Isothermal atmosphere			
MRTA with lm + N_2O	54.858	42.587	34.458
w/o-w linmix	0.000	−0.007	0.014
w/o-w N_2O	0.000	0.059	−0.120
Mid-layer T-lin τ	0.000	0.000	0.000
CKD2.1–CKD2.4	0.000	−0.216	0.600
HITRAN '96–2k	0.000	0.061	−0.132
MT_CKD–CKD2.4	0.000	−0.075	0.195

These results illustrate the magnitude of the differences among the various inputs into the monochromatic calculations. Note that the results in the first row of Table 1 can be obtained by adding the first and third rows of this table.

of magnitude smaller than the difference encountered when using the mean-layer temperature Planck function.

Fig. 5 illustrates an inter-comparison of the TOA and surface radiance calculations for the sub-arctic winter atmosphere using the same format as Fig. 4. The differences in the TOA radiances for the sub-arctic winter atmosphere are very similar, albeit somewhat smaller, than those encountered with the tropical atmosphere. For instance, neglecting the CO_2 line mixing results in a significant (10%) underestimation of the outgoing radiance at 618.5 cm^{-1}, while neglecting N_2O results in a significant (28%) overestimation of the outgoing radiance at 589.5 cm^{-1}. As noted previously, however, these discrepancies are confined to rather small spectral ranges, with the differences in the integrated radiances (see Table 2) being only −0.05% and 0.23%, respectively. Again, from an energy balance viewpoint, the most important case involves the substitution of the CKD 2.1 for the CKD 2.4 continuum, which results in the integrated TOA radiance being reduced by 0.89%.

In contrast to the TOA radiances, the inter-comparisons of the surface radiances for the sub-arctic winter atmosphere are dramatically different than those for the tropical atmosphere. In five of the

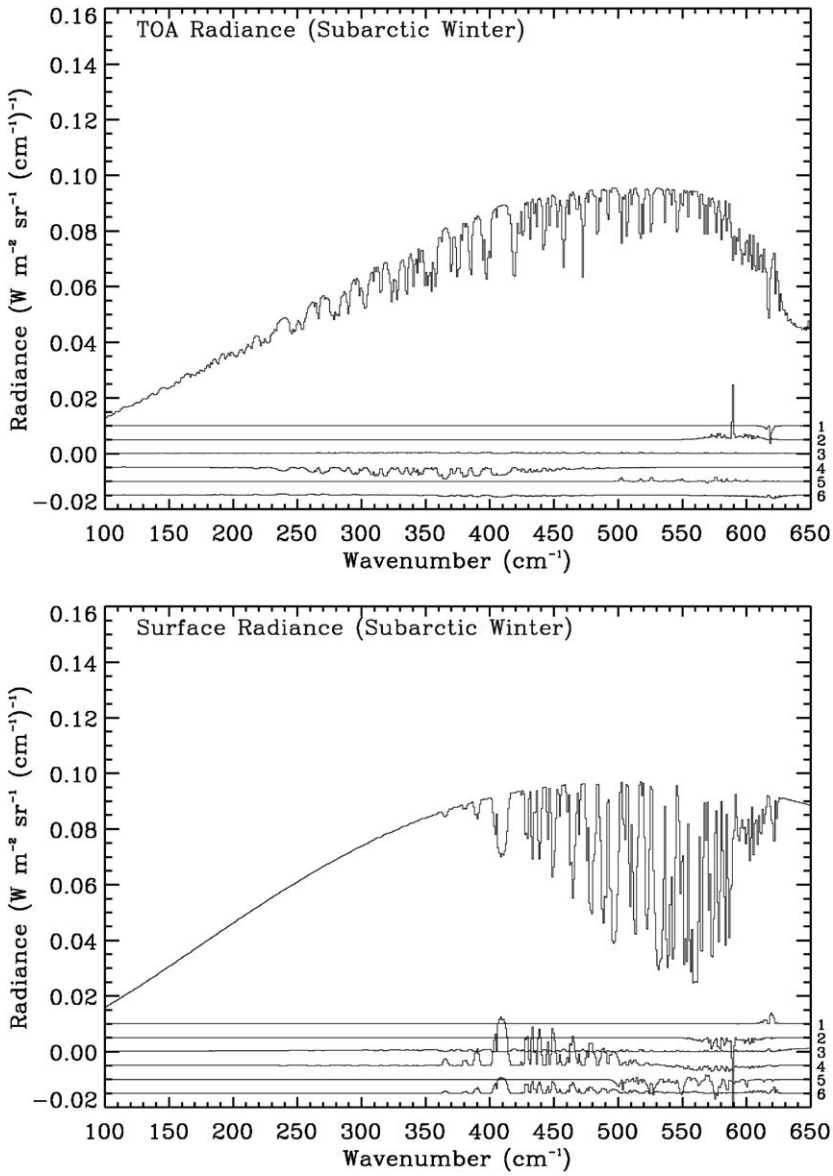

Fig. 5. A comparison of TOA and surface radiance calculations analogous to those presented in Fig. 4 except this case is for the sub-arctic winter atmosphere.

six cases only minor changes occur in the surface radiances for the tropical atmosphere; these same cases produce significantly larger discrepancies for the sub-arctic winter atmosphere. Interestingly enough, the single case which produces a noticeable discrepancy for the tropical case, i.e., substitution of the mean-layer temperature Planck function for the linear in τ approximation, causes only a small difference for the sub-arctic winter case. This is primarily due to the inversion in the

sub-arctic winter atmosphere ameliorating the discrepancy associated with the use of the mean-layer temperature Planck function approximation. The cooler, dryer sub-arctic winter atmosphere, however, being somewhat more transparent than the tropical atmosphere, substantially enhances the sensitivity of the downward surface radiances to changes in the opacity of the water vapor lines and continuum as well as increasing the impact of N_2O absorption and CO_2 line mixing. Neglecting the CO_2 line mixing causes a modest (3.6%) overestimation of the downward surface radiance at 618.5 cm^{-1}, while neglecting N_2O results in a significant (37%) underestimation of the downward surface radiance at 589.5 cm^{-1}. As before, however, these discrepancies are confined to rather small spectral ranges, and thus, the differences in the integrated radiances (see Table 2) are only 0.05% and −0.29%, respectively. Again, from an energy balance viewpoint, the most important case involves the substitution of version 2.1 of the CKD continuum code for version 2.4. This results in a 24% overestimation of the downward surface radiance at 410.5 cm^{-1} and an integrated surface radiance being enhanced by 1.31% over the 100–650 cm^{-1} range. The corresponding differences caused by substituting MT_CKD 1.0 for CKD 2.4 are 7.8% and 0.58%. A conclusive determination of the relative accuracies of these continuum formulations, however, is problematic since the uncertainties in the water vapor abundances obtained during the clear-sky periods in SHEBA prevent a clear distinction between the MT_CKD 1.0 and CKD 2.4 continua. Thus, to allow for an accurate determination of the magnitude of the water vapor continuum, future aircraft/satellite observations in the far-infrared will require very precise, of order ±5%, middle and upper tropospheric water vapor measurements [40]. The substitution of HITRAN 1996 for HITRAN 2000 produces an integrated surface radiance difference of −0.39%.

Fig. 6 illustrates an inter-comparison of the TOA and surface radiance calculations for the isothermal atmosphere using the same format as Fig. 4. The differences in the TOA and surface radiances for the isothermal and sub-arctic winter atmospheres are very similar, with the only notable differences being in the comparison of the continuum codes for the TOA calculations. These differences are caused by the isothermal atmosphere becoming opaque and therefore insensitive for wave-numbers below 350 cm^{-1}.

Contrasting the differences for the model inter-comparisons presented in Figs. 1–3 and Table 1 with the differences for the input test cases presented in Figs. 4–6 and Table 2 emphasize the relative accuracies of the models as compared to the inputs into those models. In addition, the results indicate that the cooler, dryer sub-arctic winter atmosphere provides a better test case for downward radiance inter-comparisons than the tropical atmosphere. These results, along with the results shown by Tobin et al. [5] suggest that future far-infrared inter-comparisons should include an additional high-latitude (Arctic/Antarctic) atmospheric profile.

6. Conclusions and future work

The six line-by-line models, considered in this inter-comparison, demonstrate remarkably good agreement for the three atmospheric profiles, thereby emphasizing the maturity of the high resolution modeling in the far-infrared. This maturity implies high confidence in the ability to analyze the forthcoming data from the FIRST project. The results of this study also demonstrate that differing input parameters, e.g., molecular line databases and continua formulations, can easily dominate the small residuals inherent to the different model algorithms. These conclusions are in general

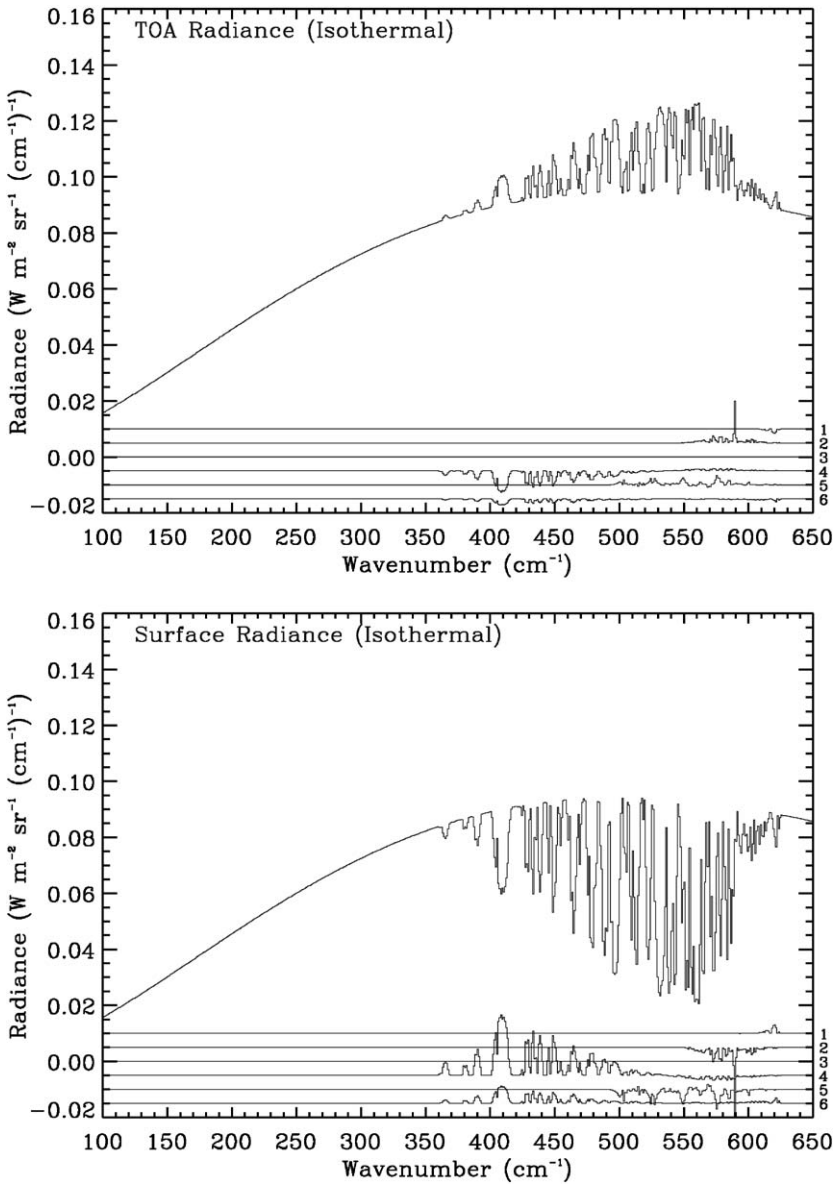

Fig. 6. A comparison of TOA and surface radiance calculations analogous to those presented in Fig. 4 except this case is for the isothermal atmosphere.

agreement with the conclusions from the ISSWG line-by-line inter-comparison [8] which considered the mid-infrared spectral range from 590 to 2700 cm^{-1}.

The results of the present study also confirm previously reported conclusions that the low absolute humidity conditions prevalent for high latitude cases can allow for the appearance of semi-transparent micro-windows in the far-infrared (see e.g., Tobin et al. [5]). Such micro-windows serve as spectral

regions of higher sensitivity to uncover differences in the model formulations. This strongly suggests that future far-infrared model inter-comparisons should include Arctic/Antarctic (North and South Pole) atmospheric profiles. The present results further suggest that CO_2 line mixing and N_2O absorption should be included in future inter-comparisons. While the inclusion of CO_2 line mixing and N_2O absorption should not be an impediment for the participation of additional high-resolution models, such requirements may prove problematic for highly parameterized models which are critical for remote sensing data analyses and operational climate studies. Indeed, one of the most significant challenges will be the inclusion of operational climate models into future far-infrared code inter-comparisons. Because of the importance of clouds in far-infrared studies [12], future model inter-comparisons will also consider cloud effects, specifically cirrus, as well as surface emissivity.

References

[1] Kratz DP. High resolution modeling of the far-infrared. Proc SPIE 2001;4485–34:171–80.
[2] Clough SA, Iacona MJ, Moncet J-L. Line-by-line calculations of atmospheric fluxes and cooling rates: application to water vapor. J Geophys Res 1992;97(D14):15761–85.
[3] Sinha A, Harries JE. Water vapour and greenhouse trapping: the role of the far-infrared absorption. Geophys Res Lett 1995;22:2147–50.
[4] Sinha A, Harries JE. The Earth's clear-sky radiation budget and water vapour absorption in the far-infrared. J Climate 1997;10:1601–14.
[5] Tobin DC, Best FA, Brown PD, Clough SA, Dedecker RG, Ellingson RG, Garcia RK, Howell HB, Knuteson RO, Mlawer EJ, Revefrcomb HE, Short JF, van Delst PFW, Walden VP. Downwelling spectral radiance observations at the SHEBA ice station: water vapor continuum measurements from 17 to 26 μm. J Geophys Res 1999;104:2081–92.
[6] Sinha A, Allen MR. Climate sensitivity and tropical moisture distribution. J Geophys Res 1994;99:3707–16.
[7] Ellingson RG, Ellis J, Fels S. The intercomparison of radiation codes in climate models: longwave results. J Geophys Res 1991;96(D5):8929–53.
[8] Tjemkes SA, Patterson T, Rizzi R, Shephard MW, Clough SA, Matricardi M, Haigh JD, Hopfner M, Payan S, Trotsenko A, Scott N, Rayer P, Taylor JP, Clebaux C, Strow LL, DeSouza-Machado S, Tobin D, Knuteson R. The ISSWG line-by-line inter-comparison experiment. JQSRT 2003;77:433–53.
[9] Mlynczak MG, Johnson D, Bingham G, Jucks K, Traub W, Gordley L, Harries J. The far-infrared spectroscopy of the troposphere (FIRST) project. Proceedings of the IEEE International Geosciences and Remote Sensing Symposium 2003, vol. 1, 2003. p. 512–4.
[10] Mlynczak MG, Harries JE, Rizzi R, Stackhouse PW, Kratz DP, Johnson DG, Mertens CJ, Garcia RR, Soden BJ. The far-infrared: a frontier in remote sensing of Earth's climate and energy balance. Proc SPIE 2001;4485-34:150–8.
[11] Brindley HE, Harries JE. The impact of far i.r. absorption on clear sky greenhouse forcing: sensitivity studies at high spectral resolution. JQSRT 1998;60:151–80.
[12] Yang P, Mlynczak MG, Wei H, Kratz DP, Baum BA, Hu YX, Wiscombe WJ, Heidinger A, Mishchanko MI. Spectral signature of cirrus clouds in the far-infrared region: single-scattering calculations and radiative transfer sensitivity studies. J Geophys Res 2003;108(D18):4569.
[13] Clough SA, Kneizys FX, Shettle EP, Anderson GP. Atmospheric radiance and transmittance. Sixth Conference on Atmospheric Radiation, American Meteorological Society, Boston, MA, 1985. p. 141–4.
[14] McClatchey RA, Fenn RW, Selby JE, Volz FE, Garing JS. Optical properties of the atmosphere, 3rd ed. AFCRL-72-0497, Environmental Research Papers No. 411, Air Force Cambridge Research Laboratory, Bedford, MA, 1972.
[15] Rothman LS, Barbe A, Benner DC, Brown LR, Camy-Peyret C, Carleer MR, Chance K, Clerbaux C, Dana V, Devi VM, Fayt A, Flaud J-M, Gamache RR, Goldman A, Jacquemart D, Jucks KW, Lafferty WJ, Mandin J-Y, Massie ST, Nemtchinov V, Newnham DA, Perrin A, Rinsland CP, Schroeder J, Smith KM, Smith MAH, Tang K, Toth

RA, Vander Auwera J, Varanasi P, Yoshino K. The HITRAN molecular spectroscopic database: edition of 2000 including updates of 2001. JQSRT 2003;82:5–44.

[16] Rothman LS, Rinsland CP, Goldman A, Massie ST, Edwards DP, Flaud J-M, Perrin A, Camy-Peyret C, Dana V, Mandin J-Y, Schroeder J, McCann A, Gamache RR, Wattson RB, Yoshino K, Chance KV, Jucks KW, Brown LR, Nemtchinov V, Varanasi P. The HITRAN molecular spectroscopic database and HAWKS (HITRAN Atmospheric Workstation): 1996 edition. JQSRT 1998;60:665–710.

[17] Clough SA, Kneizys FX, Davies RW. Line shape and the water vapor continuum. Atmos Res 1989;23:229–41.

[18] Mlawer EJ, Clough SA, Brown PD, Tobin DC. A new formulation for the water vapor continuum. Eighth ARM Science Team Meeting, Atmospheric Radiation Measurement Program, Tuscon, AZ, 1998.

[19] Revercomb HE, Best FA, Dedecker RG, Dirks TP, Herbsleb RA, Knutson RO, Short JF, Smith WL. Atmospheric emitted radiance interferometer (AERI) for ARM. Fourth Symposium on Global Climate Change Studies, American Meteorological Society, Anaheim, CA, 1993. p. 46–9.

[20] Turner DD, Tobin DC, Clough SA, Brown PD, Ellingson RG, Mlawer EJ, Knuteson RO, Revercomb HE, Shippert TR, Smith WL, Shephard MW. The QME AERI LBLRTM: a closure experiment for downwelling high spectral resolution infrared radiance. J Atmos Sci 2003, accepted for publication.

[21] Clough SA, Iacono MJ. Line-by-line calculations of atmospheric fluxes and cooling rates, 2: application to carbon dioxide, ozone, methane, nitrous oxide and the halocarbons. J Geophys Res 1995;100(D8):16519–35.

[22] Mlawer EJ, Taubnam SJ, Brown PD, Iacono MJ, Clough SA. RRTM, Radiative transfer for inhomogeneous atmospheres: a validated correlated-k model for the longwave. J Geophys Res 1997;102:16663–82.

[23] Morcrette J-J, Clough SA, Mlawer EJ, Iacono MJ. Impact of a validated radiative transfer scheme, RRTM, on the ECMWF climate model and 10-day forecasts, ECMWF Research Department Technical Memo No. 252, 1998. p. 47.

[24] Iacono MJ, Mlawer EJ, Clough SA, Morcrette JJ. Impact of an improved longwave radiation model, RRTM, on the energy budget and thermodynamic properties of the NCAR community climate model CCM3. J Geophys Res 2000;105:14873–90.

[25] Warner JX, Ellingson RG. A new narrowband radiation model for water vapor absorption. J Atmos Sci 2000;57: 1481–96.

[26] Gordley LL, Marshall BT, Chu DA. LINEPAK: algorithms for modeling spectral transmittance and radiance. JQSRT 1994;52:563–80.

[27] Mertens CJ. Feasibility of retrieving upper tropospheric water vapor from observations of far-infrared radiation. Proc SPIE 2001;4485-34:191–201.

[28] Miskolczi F, Bonzagni M, Guzzi R. High-resolution atmospheric radiance-transmittance code HARTCODE. Meteorology and environmental sciences. Singapore: World Scientific, 1990. p. 743–90.

[29] Martin-Torres FJ, Kutepov A, Gusev O, Dudhia A, Lara LM, Feofilov AG, Lopez-Puertas M, Taylor FW. A non-LTE model for the atmosphere of Titan and implications for the Cassini CIRS experiment. Geophysical Research Abstracts 5, EAE03-A-07023, 2003.

[30] Martin-Torres FJ, Kutepov A, Dudhia A, Gusev O, Feofilov AG. Accurate and fast computation of the radiative transfer absorption rates for the infrared bands in the atmosphere of Titan. Geophysical Research Abstracts 5, EAE03-A-07735, 2003.

[31] Edwards DP. GENLN2. A general line-by-line atmospheric transmittance and radiance model Version 3.0. NCAR Technical note NCAR/TN-367+STR, National Center for Atmospheric Research, Boulder, CO, 1992.

[32] Brindley HE, Geer AJ, Harries JE. Climate variability and trends in SSU radiances: a comparison of model predictions and satellite observations in the middle stratosphere. J Climate 1999;12:3197–219.

[33] Collins WD, Hackney JK, Edwards DP. An updated parameterization for infrared emission and absorption by water vapor in the National Center for Atmospheric Research community atmosphere model. J Geophys Res 2002;107(D22):4664. doi:10.1029/2001JD001365.

[34] Kratz DP, Chou M-D, Yan M-H, Ho C-H. Minor trace gas radiative forcing calculations using the *k* distribution with one-parameter scaling. J Geophys Res 1998;103:31647–56.

[35] Kratz DP, Rose FG. Accounting for molecular absorption within the spectral range of the CERES window channel. JQSRT 1999;61:83–95.

[36] Kratz DP, Priestley KJ, Green RN. Establishing the relationship between the CERES window and total channel measured radiances for conditions involving deep convective clouds at night. J Geophys Res 2002;107(D15):4245. doi:10.1029/2001JD001170.
[37] Mlawer EJ, Tobin DC, Clough SA. The MT-CKD water vapor continuum: A revised perspective including collision induced effects, Atmospheric Science from Space using Fourier Transform Spectrometry II Workshop, Bad Wildbad, Germany, 2003.
[38] Wiscombe WJ. Extension of the doubling method to inhomogeneous sources. JQSRT 1976;16:477–89.
[39] Fu Q, Liou KN. Parameterization of the radiative properties of cirrus clouds. J Atmos Sci 1993;50:2008–25.
[40] Harries JE. Atmospheric radiation and atmospheric humidity. Q J R Meteorol Soc 1997;123:2173–86.